

Technical Aspects of Larmor Precession with Inclined Front and End Faces

M.Th. Rekveldt, W.G. Bouwman, W.H. Kraan, O. Uca, S.V. Grigoriev, and R. Kreuger

Interfacultair Reactor Instituut, Delft University of Technology, Mekelweg 15, 2629 JB Delft, the Netherlands

Abstract. Some technical and physical features of Larmor precession techniques will be discussed. Various options to encode the transmission angle of the neutron beam by inclined front and end faces using DC fields are considered, under which magnetized foils and wedge shaped precession regions. The use of shaped pole faces as precession regions to avoid material in the transmitted beam are considered together with correction methods for the inhomogeneous field line integrals accompanied by those magnetic fields. It appears that the use of π flippers as occurring in the resonance method are of great advantage.

Introduction

The instruments discussed in the previous chapter by Rekveldt *et al.* all are based on Larmor precession of polarized neutrons. We will concentrate in this chapter on experimental details, essential for generating field line integrals, homogeneous over the cross-section of the beam. First we will consider different options to realize inclined front and end faces. After that we will consider the field line integrals, the inhomogeneities of them over the cross-section of the beam and how to get them homogeneous. Some experimental results of correction systems built up to now will be shown.

1 Options to Realize Inclined Faces

The methods to create Larmor precession regions with inclined front and end faces can be divided in two classes: The classical Larmor precession in a constant magnetic field and the neutron resonance technique with radio frequency (RF) fields. We applied two different techniques with the classical Larmor precession: real triangularly shaped pole shoes and rectangularly shaped pole shoes with magnetized foils to start and to stop the precession. In both cases the precession regions were in fact two oppositely oriented triangularly shaped regions and not parallelogram shaped as indicated in the previous chapter as shown in Fig. 1. Shaping the field regions as triangles means that the precession occurring in the central regions, marked light gray in the figure, is omitted. This will not affect the property of these precession regions that the precession angle depends on the transmission angle. This reduces the inelastic scattering contribution to the spin

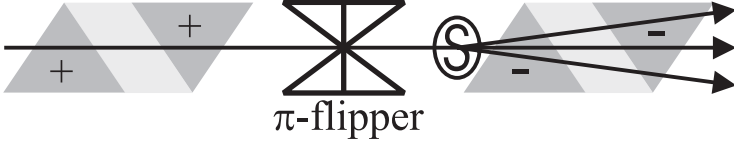


Fig. 1. Schematic side view of a setup with triangularly shaped precession regions. The dark gray areas are symbols for the triangularly shaped precession regions. Two triangles together act as a parallelogram with the middle (indicated with light gray) removed. The magnetic field in the last two magnets is opposed to the field in the first two magnets. In the middle of the setup is a π flipper.

echo signal. We discuss also two different methods with the neutron resonance techniques in which the precession regions are parallelogram shaped. These two methods will therefore have a larger sensitivity to inelastic scattering.

The property of a precession device with inclined faces that it encodes the transmission angle of a neutron trajectory, entails that such a device cannot be tested directly or only with a very narrow divergent beam. Testing occurs always in spin echo mode, with an echoing precession device of equal geometry.

1.1 Triangular Shaped Pole Shoes

The simplest option is to use triangularly shaped magnetic pole shoes as depicted in Fig. 2. Setting four of these magnets in a line with a π flipper in the middle constitutes a simple SESANS [1] setup (Fig. 1). This turns out indeed to be a rather simple method to obtain a good spin echo as shown in Fig. 3. A polarization of 0.8 is achieved in a rather preliminary setup for both the white and the monochromatic beam. An advantage is that the triangles produce an echo for a white spectrum. A disadvantage is that there are many field transition regions which may give rise to depolarization of the beam.

1.2 Magnetized Foil

As another option to realise triangularly shaped precession regions [2] we use a foil (see Fig. 4a) of a soft magnetic material [3] placed between the poles of an electromagnet and magnetized to saturation. The applied magnetic field B_{ext} results inside the foil in a local saturated induction B_s in the plane of the foil. This local strong magnetic field is very convenient for manipulating the neutron polarization. The neutron in the foil is subjected to an effective field B_{eff} which is the vector sum of the local induction B_s (defined with the vertical angle θ_0) and the applied external field B_{ext} as shown in Fig. 4a. The value of the field is

$$B_{\text{eff}} = \sqrt{(\cos(\theta_0)B_s)^2 + (\sin(\theta_0)B_s + B_{\text{ext}})^2} \quad (1)$$

and its angle with the horizontal axis is

$$\theta_{\text{eff}} = \cot \left(\frac{\cos(\theta_0)B_s}{\sin(\theta_0)B_s + B_{\text{ext}}} \right). \quad (2)$$

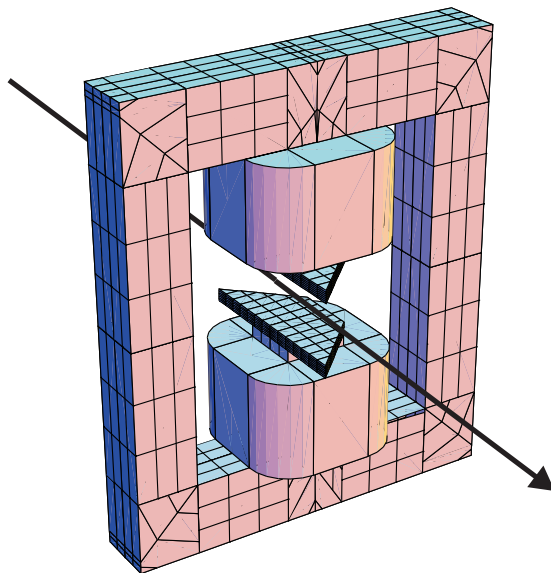


Fig. 2. Schematic drawing of a precession device with triangularly shaped pole shoes. The rectangle is a yoke for the electromagnet. The triangularly shaped pole shoes are mounted on solid iron poles. Electrical coils are wound around the poles. The arrow indicates the neutron path through the magnet. The same magnets have been used in all experiments, but with differently shaped pole shoes and sometimes with foils or extra coils inside the pole gap.

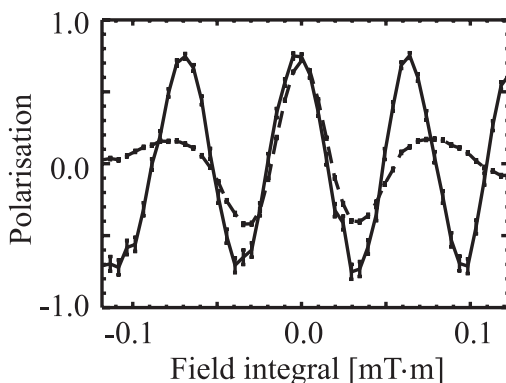


Fig. 3. Spin echo obtained with a wedge setup. The echo of the polarization is observed by scanning the strength of the guide field in one of the arms of the instrument. The drawn line describes the polarization change of a beam with a wavelength $\lambda = 0.204$ nm and a width and height of 5×5 mm². The applied magnetic field in the magnets was $B = 0.06$ T. The dashed line represents the polarization of the white thermal beam which has a peak at $\lambda = 0.16$ nm. The polarization in echo of the white beam is as good as of the monochromatic beam. This is an advantage of the wedge option.

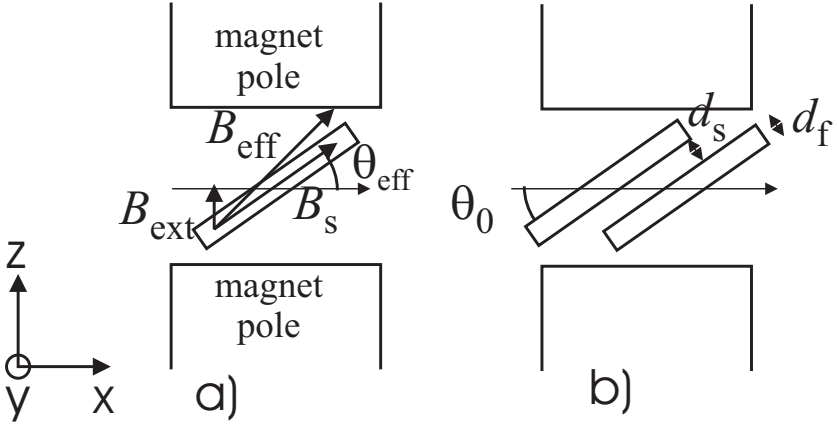


Fig. 4. Schematic side view diagram of a magnetized foil a) and double foil b) with a graphic definition of the symbols used in the text.

The polarization vector rotates in the foil over an angle

$$\phi_f = c\lambda B_{\text{eff}} d_f / \sin(\theta_0) \quad (3)$$

around this local induction, in which $d_f / \sin(\theta_0)$ is the path length through the magnetized foil and c a constant determined by the magnetic moment of the neutrons ($c = 4.6368 \cdot 10^{14} \text{T}^{-1} \text{m}^{-2}$). The rotation matrix R_f for the polarization vector can be calculated from these parameters.

When we calculate the precession inside the foil with the matrix R_f acting on the initial polarization in the z -direction, we find that the polarization is turned into the horizontal plane, perpendicular to the applied field if a proper thickness d_f of the foil has been chosen. As a consequence, the Larmor precession starts after the foil. The precession continues until the end of the field between the poles of the electromagnet which is perpendicular to the neutron beam. Thus a triangular precession region is created.

Two parallel foils spaced by a distance d_s (shown in Fig. 4b) can function as a spin mirror by rotating the polarization by π radians around the x -axis. The transformation of the polarization vector is composed of three rotations: a rotation ϕ_f around the magnetization in the first foil, next a rotation in the space between the foils ϕ_s around the vertical magnetic field B , and finally again a rotation ϕ_f around the magnetization in the second foil. The rotation between the foils is over an angle

$$\phi_s = c\lambda B_{\text{ext}} d_s / \sin(\theta_0) \quad (4)$$

which is described by a rotation matrix R_s . So, the matrix due to the double foil can be calculated:

$$R_d = R_f R_s R_f. \quad (5)$$

The rotation in the space between the foils can be tuned by varying B or d_s . The importance of the double foil is that it now works as a mirror in the xz -plane.

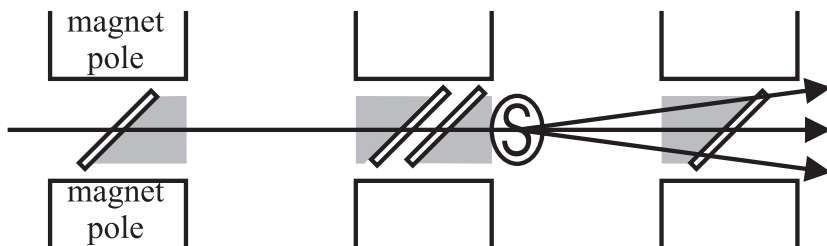


Fig. 5. Schematic side view diagram of a SESANS setup built with magnetized foils. The spin echo length z can be varied by changing the sample (denoted with the “S”) position. The gray areas indicate the precession regions. All the magnetic fields in the setup point in the same direction.

By positioning successively a single foil, a double foil and a single foil at equal distances, a spin echo set-up is obtained with triangular precession regions as indicated in Fig. 5. The first single foil turns the polarization into the horizontal plane, thus starting the precession. The double foil mirrors the polarization in the horizontal plane which effectively reverses the direction of the precession. The last single foil turns the polarization back into the yz plane, which stops any precession that would change the vertical component of the polarization P_z . This setup can directly be used for SESANS experiments as presented in the previous chapter [1]. An echo obtained with this geometry is presented in Fig. 6. The polarization in this case in the echo condition is 0.8 for the monochromatic beam. For the white spectrum the foils do not work as effectively and the polarization is only 0.5. This makes the foil option not suitable for application at a pulsed source. A great advantage of SESANS with foils is the sharp definition of the geometry of the precession regions. Another advantage is that all magnetic fields point in the same direction, which facilitates the magnetic field construction.

1.3 Neutron Spin Resonance Precession with Step DC Field

We now proceed to the resonance techniques to create the precession of neutron spins. The principle of this technique is based on the essential difference of position dependent and time dependent potentials for neutrons. Although in general precession of neutron spins in a DC magnetic field is described as precession in time, it is in fact precession in space and not in time. Precession in space is described by the splitting of the k -vector in k^+ and k^- for the two spin states, which happens because the two spin states are accelerated and decelerated upon entering the magnetic field (Fig. 7). This splitting describes the precession rate [4,5,6,7]. Using the time dependent resonance field to flip the neutron spin in the magnetic field the total energy of the neutrons changes but not its kinetic energy, thus without changing the k vectors. This spin reversal creates doubling of the k -splitting after leaving the field (see Fig. 7).

Up to now the neutron spin resonance precession has been applied using local DC fields, created by a DC current in a coil wound around the resonance coil

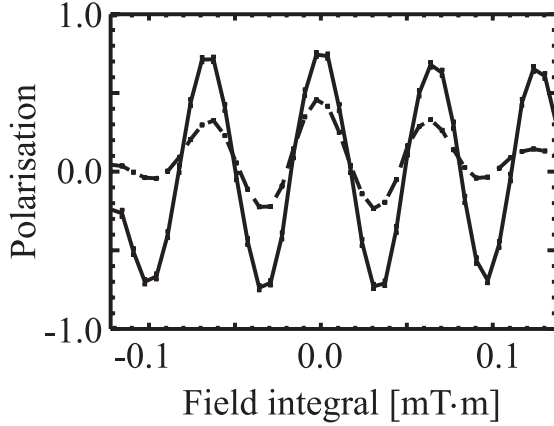


Fig. 6. Spin echo obtained with a foil setup. The echo of the polarization is observed by scanning the field in a guide field in one of the arms of the instrument. The drawn line describes the polarization change of a beam with a wavelength $\lambda = 0.204$ nm and a width and height of 5 by 5 mm². The foils consist of CoFeNi with a thickness $d_f = 23$ μ m and have a magnetization of 1 T. The foils have an angle of $\vartheta_0 = 41^\circ$ with the horizontal plane. The external applied field was $B_{\text{ext}} = 0.07$ T. The space between the foils in the double foil was 0.2 mm. The dashed line represents the polarization of the white thermal beam which has a peak at $\lambda = 0.16$ nm. The echo of the white beam is much lower, since the foils work only well for one specific wavelength.

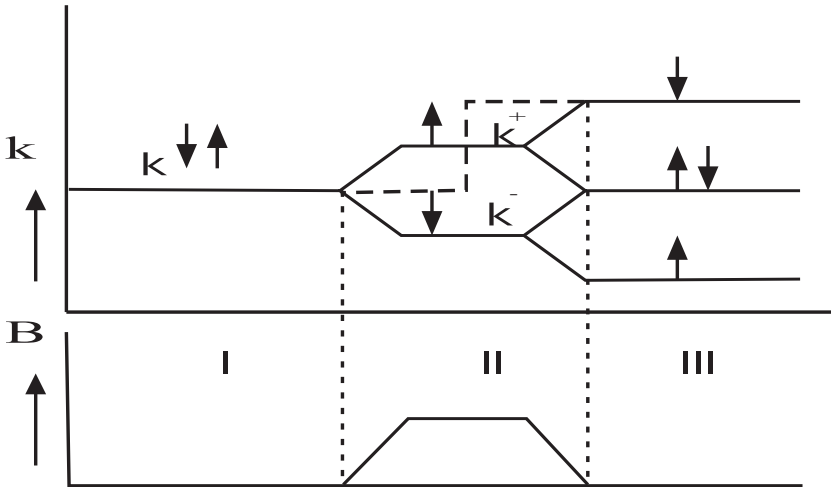


Fig. 7. Splitting of the k vector (top figure) of a neutron beam when entering and leaving a magnetic field (bottom figure). Entering the field by going from region I to II, the two neutron spin states are accelerated and decelerated respectively and thus the corresponding wave vectors are split up. Leaving the field by going from region II to III, this splitting disappears again as one expects (central level in region III). However when one reverses the spin in the field the effects of accelerating and decelerating reverses too and the splitting of the k -vectors is doubled arriving in region III (top and lower level in region III).

[5], occurring for the neutron as a step function. In this way field components deviating from the main field direction caused by field gradients are avoided which is an important condition for homogeneity of the field line integrals. Doing this one accepts that material of the magnet and resonance coils disturbs the neutron beam passing through the system, which can be a serious problem in small angle scattering. This last fact limits the achievable field with conventional aluminum coils to about 200 Gauss. Another advantage of this geometry is that it facilitates the creation of inclined front and end faces. To understand this, one should realise that the Larmor precession is just equal to the line integral of the splitting of the k vectors for the + and - spin direction. The effective starting point of the neutron spin resonance precession is the symmetry plane of the DC fields in which the spin was flipped. This becomes clear when one considers in Fig. 7 the area of the region where the k vectors for the + and - spin are different. That area is equal to the area, determined by the symmetry planes through the DC field indicated in the same figure by a broken line,. So this symmetry plane in each DC field determines actually the starting and ending point of the neutron spin resonance Larmor precession. This fact is of paramount importance and plays an important role in reducing effects of line integral inhomogeneities.

1.4 Neutron Spin Resonance Precession with a White Neutron Spectrum

In this section we will describe the use of an electromagnet together with a resonance coil, flipping the whole wavelength spectrum of a neutron beam without any interference of material with the transmitted neutron beam. The latter is achieved by letting the beam pass between the poles of the electromagnet and using a resonance coil shaped as a solenoid with axis parallel to the neutron beam direction. As a consequence of the fact that the fields increase or decrease along the neutron path we get line integral gradients. Figure 8 shows a sketch of the field and k -splitting as function of x in one arm of the spin echo setup. Figure 9 shows a top view of the whole spin echo setup indicating the inclined front and end faces of the precession regions. Note the gradient of the DC -field around the resonance field (see top of Fig. 8). This gradient together with the alternating field amplitude B_{coil} in the resonance coil, cause in the reference frame (middle figure in Fig. 8), rotating with the resonance frequency ω_{res} , a net field slowly changing from the positive z , via the x' direction in the rotating frame, to the negative z -direction. The neutron spin will follow this direction adiabatically for all wavelengths above a certain wavelength, determined by the ration $r = \omega'_L/\omega_g$, where ω'_L is the Larmor frequency defined in the net DC field of the reference system and ω_g the geometric frequency representing the speed with which the field changes its direction from $+z$ to $-z$ along the x -direction. The spin flip probability ρ in such gradient field is approximated by

$$\rho = 1 - \frac{1}{2(r^2 + 1)}. \quad (6)$$

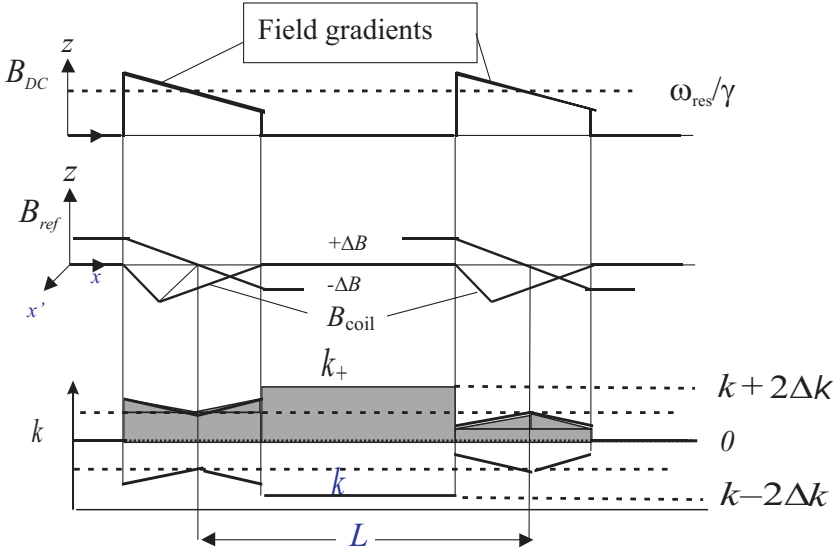


Fig. 8. Diagram of the k -splitting in the resonant spin echo mode using a DC magnetic field B between magnetic poles and DC gradient fields of amplitude ΔB (top figure). Further an alternating field with frequency ω and an amplitude of B_{coil} is used. In the rotating frame with frequency ω the neutron experiences a slowly varying field in the z -direction from the $+\Delta B$ to $-\Delta B$ and in the x' direction a slowly increasing and then decreasing field with amplitude B_{coil} . (central figure). These fields together can be considered as a rotating field around the x' direction, in which the neutron spin follows adiabatically. This creates a perfect spin reversal for all neutron wavelength above some critical value, depending on the geometrical speed of field change.

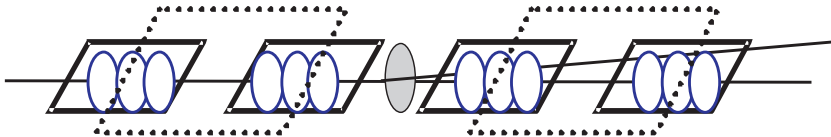


Fig. 9. Top view of zero-field precession setup using 4 magnetic parallelogram shaped pole gaps (indicated with the drawn black lines) with 4 resonance coils (indicated with the ellipses) between the gaps. The parallelogram-shaped pole shoes cause the inclined front and end faces of the precession regions. The symmetry planes defined by the pole shoes, define also the effective start and end points of the precession regions (indicated with the dashed lines). A sample (indicated as the gray ellipse) can be positioned in the middle of the setup to study SESANS.

Test experiments with this set-up have been performed with the set-up shown in Fig. 9 at DC fields of 760 Gauss. A field coil generating an extra DC field was placed between the SE-arms, in order to measure the precise phase around the spin echo point. The setup can be used with the resonant flipper switched off (DC mode) and on (RF mode). Figure 10 shows measuring results for the flipping probability of the 4 flippers in series. The left figure gives the wavelength spectra

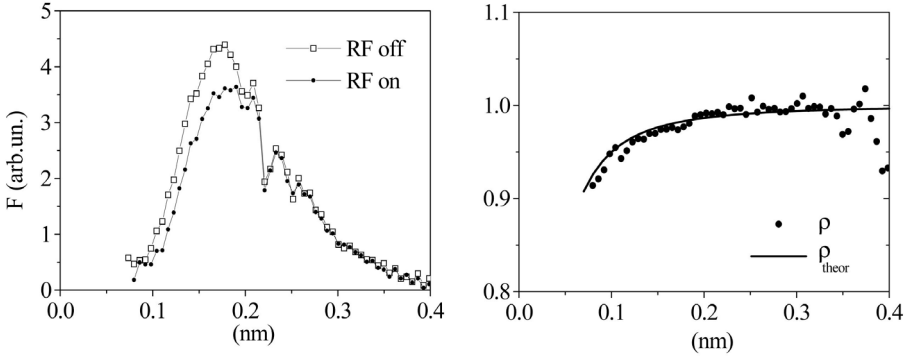


Fig. 10. Measured wavelength spectra without and with the 4 spin flippers switched on (left). Division of the two spectra yields the effective flipping probability of the 4 flippers (right).

measured with the 4 spin flippers switched on and off. The flipping probability of the flipper is found by dividing the two spectra by each other, according to formula

$$\rho = \frac{1}{2} \left(1 + \sqrt[4]{\frac{F_{on}}{F_{off}}} \right) \quad (7)$$

that has been plotted in the right of Fig. 10. The theoretical calculated spin-flip probability is indicated as a line.

The sensitivity of the setup for variations of the DC field in DC mode and in the resonant (RF) mode have been investigated and are presented in Fig. 11. The linear dependence of the phase in the DC mode is obvious and the insensitivity of the RF mode against the DC field variation is just as expected. The phase should be sensitive only to the frequency used and not to the field used to get resonance. Another interesting feature investigated is the sensitivity of the phase to variation of the gradient field used to get flipping of the white beam. From Fig. 8 one sees that the effect of the gradient field in one magnet cancels in the DC mode and gives some net rotation in the RF mode. This is indeed observed as shown in Fig. 11. One may note from Fig. 8 that in the RF mode, variations of B_{grad} in two coils will give likewise no net precession.

2 Technical Details for Homogeneous Field Line Integrals

It is clear that in any precession device the homogeneity of the field line integrals over the cross-section of the beam is very important [8]. In spin echo devices up to now, fields are used about parallel to the neutron paths. In that case, the homogeneity requirement is solved by constructing Fresnel current lenses, in cylindrical symmetry, around the beam axis. Such a correction procedure is impossible when one requires strong inclined front and end faces of the precession

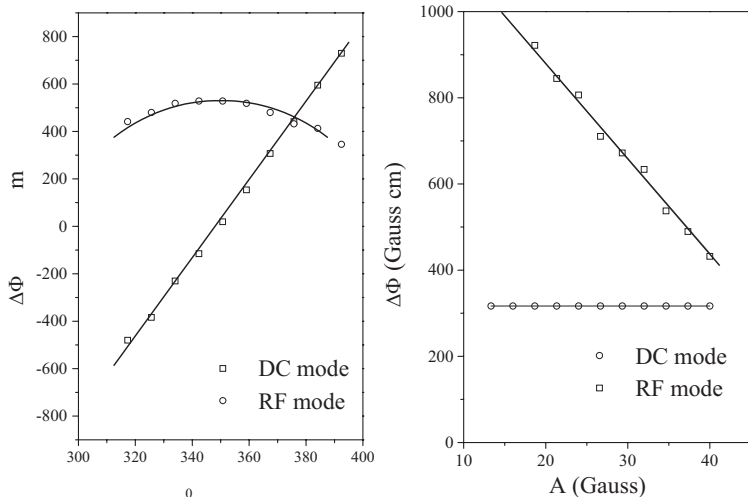


Fig. 11. Sensitivity of the precession angle φ for variations of the DC field. B^{res} is measured in DC mode and RF mode (left). The little down bending of the $\Delta\varphi$ in the RF mode is ascribed to decreasing flipping probability out of optimum resonance field. Sensitivity of the precession phase $\Delta\varphi$ for variations of the amplitude of the gradient field B_{grad} (right). As expected the DC mode is insensitive for amplitude variations while the RF mode varies with this amplitude.

devices. This requirement forces the choice of fields perpendicular to the neutron beam.

Here we will discuss a number of possibilities to correct for the inhomogeneities in line integrals [9]. For this purpose we limit ourselves to the use of magnetic pole faces, creating a field in the z -direction and having a triangular shape in the xy -plane, as discussed above. Figure 12 (top) shows the side view of such magnetic poles. Figure 12 (bottom) shows schematically how the field components in the z - and x -direction behave in such geometry.

Applying Maxwell laws we can learn already some simple important facts about the line integrals and the field geometry. First the neutron feels the line integral $L(y, z)$ of the magnitude of the field over the cross-section of the beam in the y - and z -direction:

$$L(y, z) = \int |B(x, y, z)| dx. \quad (8)$$

If we assume that the field changes only in two directions (i.e. the magnetic poles have “infinite” length in the y -direction), namely along the z and the x' axis perpendicular to the pole gap (see Fig. 12), we can write for $B_x \ll B_z$

$$|\mathbf{B}(x, z)| = \sqrt{(B_z^2 + B_x^2)} \approx B_z \left(1 + \frac{B_x^2}{2B_z^2}\right). \quad (9)$$

When one assumes that the medium is infinite in the y -direction, we know from flux conservation that the line integral along the x -direction of the z -component

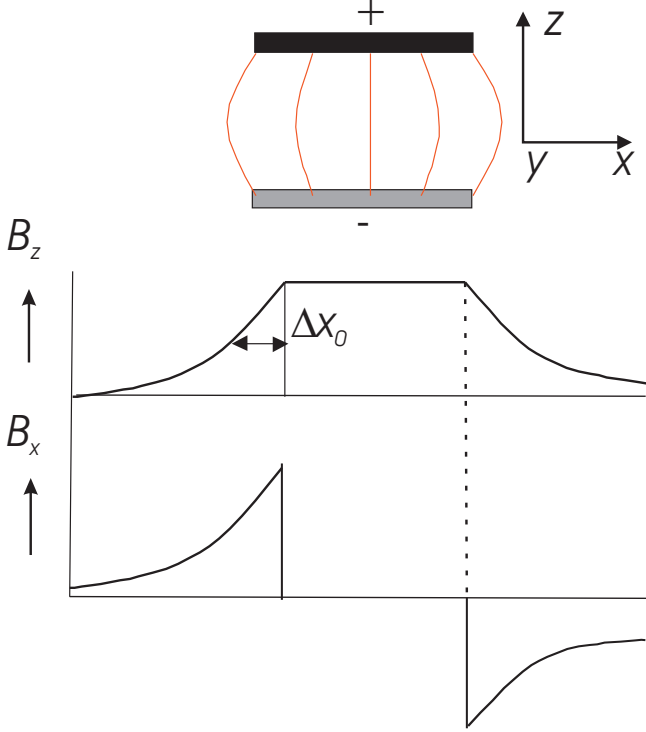


Fig. 12. Schematic view of field dependence between magnetic poles (top figure). The bottom figures show schematically how the z - and x -component of the fields change along the x -direction.

is homogeneous in the z -direction. So the deviations of the line integral $\Delta L(z)$ are only due to the x -components of the field

$$\Delta L(z) \equiv L(z) - L(0) = \int \frac{B_x^2(x)}{2B_z(x)} dx. \quad (10)$$

Using further the Taylor expansion of $B_x(x, z)$ and Maxwell's law $\nabla \times \mathbf{B} = 0$, which means $\frac{\partial B_x(x, z)}{\partial z} = \frac{\partial B_z(x)}{\partial x}$, we get

$$B_x(x, z) = B_x(x, 0) + \frac{\partial B_x(x, z)}{\partial z} z = \frac{\partial B_z(x)}{\partial x} z \quad (11)$$

and

$$\Delta L(z) = \int dx \frac{\left(\frac{dB_z(x)}{dx} z \right)^2}{2B_z(x)}. \quad (12)$$

To have a better understanding of this expression we describe the field transition entering from outside into the field region between the poles by $B_z(x) = B_0 \exp[-x/\Delta x_0]$ where Δx_0 is the half width of the transition region and B_0 the

maximum field value in the core of the magnet. Then for one field transition

$$\Delta L(z) = B_0 \frac{z^2}{2\Delta x_0}. \quad (13)$$

This simple treatment makes clear that the deviations in the line integrals go quadratically with the height z out of the symmetry plane along x and inversely proportional to the transition region over which the field drops to zero.

We will consider three different methods to homogenise the line integrals, first, eliminating the x -components of the fields, second correcting the line integral with another disturbance working in the opposite direction and thirdly using π flippers in the main fields in the symmetry planes of the fields to cancel deviations in line integral occurring symmetrically on both sides of the symmetry planes. Use of neutron spin resonance precession incorporates such an automatic compensation already around the spin flippers. We will discuss these methods shortly.

2.1 Eliminating the x-Components of the Fields

Because the x -component is the cause of the non homogeneity of the line integrals in eq. 10, it looks promising to compensate this component of the fields directly. An x -component of the field can be generated by a current in the y -direction (y -current). Any profile of x -field along the x -axis can be generated by a distribution of y -currents along the x -axis. Let us suppose that we are able to compensate the B_x component fully over a certain z range then in that range we will have $\frac{dB_x(x,z)}{dz} = 0$. Then using Maxwell's equation $\nabla \times B = 0$ in the absence of magnetization or currents, that would mean for the z -component of the field,

$$B_z(x) = \int_{-\infty}^x dx' \frac{dB_z(x', z)}{dx'} = \int_{-\infty}^x dx' \frac{dB_x(x', z)}{dz} z = 0. \quad (14)$$

This is a trivial solution we do not want, since we need the high z -component of the field. So compensating the x -field by currents does not work.

2.2 Correcting the Line Integral

First it should be noted that the line integral differences along the z -direction can be minimized according eq. 10 and eq. 13 by minimising the field component B_x or maximising the transition region Δx_0 [9]. Because the contribution to the line integral is a square of B_x , it helps to build a slowly increasing and decreasing main field B_z because $B_x \propto dB_z/dx$. Next we are going to compensate the rest of the line integral deviation on different heights by adding to the integral an opposite gradient in line integral. The system of (2×2) current wires parallel to the x -direction with positive currents at the positions (y_0, z_0) , $(y_0, -z_0)$ and negative currents in the $(-y_0, z_0)$, $(-y_0, -z_0)$, create a field in the z -direction, decreasing with z^2 and just opposite to the gradient created by the main field

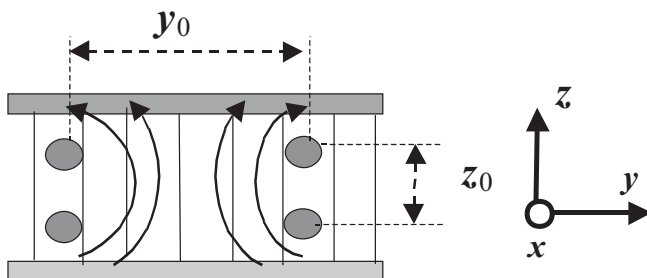


Fig. 13. Sketch of the field correction by currents parallel to the x - direction. these currents create a field line integral gradient just quadratically opposite to the gradient by the main field.

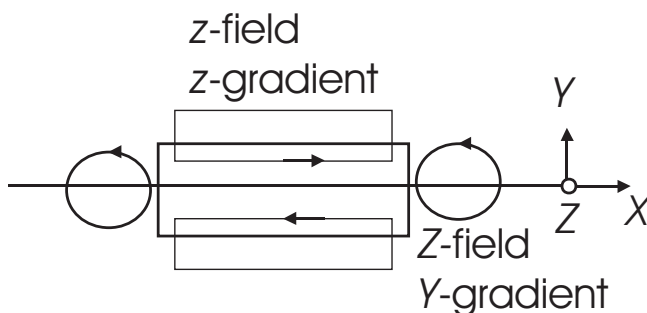


Fig. 14. Top view of current corrections. The currents in the x -direction create the gradient in the line integral in the z - and y -direction, while the circular currents in the x, y -plane create only the gradient in the y -direction.

(see Fig. 13). By choosing the correct current and $z_0 = 0.32 y_0$, the z gradient of the field is homogeneous in the y -direction and can be adjusted so that the line integral in the z -direction is fully compensated. However by doing this we just created by these correction windings also an homogeneous gradient in the y -direction, that has to be compensated in another way. The latter can not be done by shaping the pole gaps such to compensate for the line integral gradient in the y -direction, because that would increase the z -gradient proportionally. The created y -gradient can only be compensated by parabolically shaped coils with the field in the z -direction according to Fig. 14.

Measurements have been carried out up to now only with the first type of correction and using a neutron diaphragm narrow in the y -direction [8], in order to minimise the effect of the resulting gradient in the y -direction. Results of these experiments are given in Fig. 15.

The maximum polarization observed at $I = 0.55$ A in this figure corresponds to the maximum polarization that is depolarized already by other reasons. This means that the line integrals are indeed homogenised with respect to z .

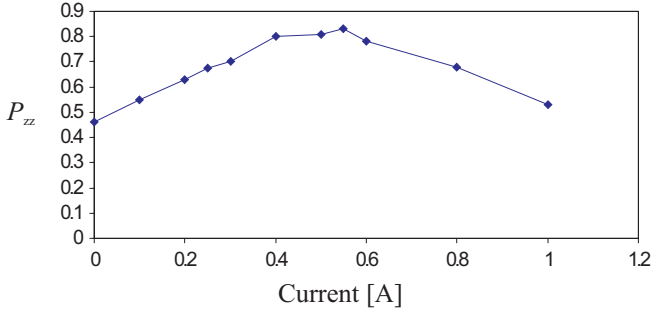


Fig. 15. Measurement of the polarization as function of the correction current I_x . The top value of the polarization corresponds to the maximum polarization achieved using a very narrow beam.

2.3 Using Neutron Spin Resonance Precession as a π -Flipper

Using this technique, we create a symmetry plane, just through the center of the magnet containing the resonance coil for spin flip. This plane determines the effective start and end positions of the precession as mentioned above. Figure 7 shows a sketch of the splitting of the k -vector causing the net precession angle. In the sketch it is shown that the symmetry plane through the magnet renders the effective starting position of the Larmor precession to first order independent of any inhomogeneity of the line integral over the cross-section of the beam. However some asymmetries arise from the divergence of the neutron beam, that makes that different parts of the symmetric fields are crossed on the left and right side of the symmetry plane. This effect can be estimated to cause line integral deviations according to

$$\Delta L = \frac{B_0}{2\Delta x_0}(z_2^2 - z_1^2) \text{ with } z_2 - z_1 = \alpha(x_0 + \Delta x_0) \quad (15)$$

where α is the divergence of the beam in the z -direction and x_0 the distance between the two transition regions on both sides of the magnet. Evaluation of this equation leads to

$$\Delta L = \frac{B_0}{\Delta x_0} z \alpha (x_0 + \Delta x_0) \quad (16)$$

which is of the order of 5 % of the effect without resonance, dependent on the actual shape and length of the magnet.

Figure 16 shows measuring results of the spin echo of (2x2) DC-magnets (top) and the same magnets with a resonance coil (bottom) in it. The DC measurements show strong depolarization at the field values of 365 Gauss (left-hand figures) and 760 Gauss (right-hand figures), while the resonance mode (RF in figure) shows only a little difference in depolarization at the two field values.

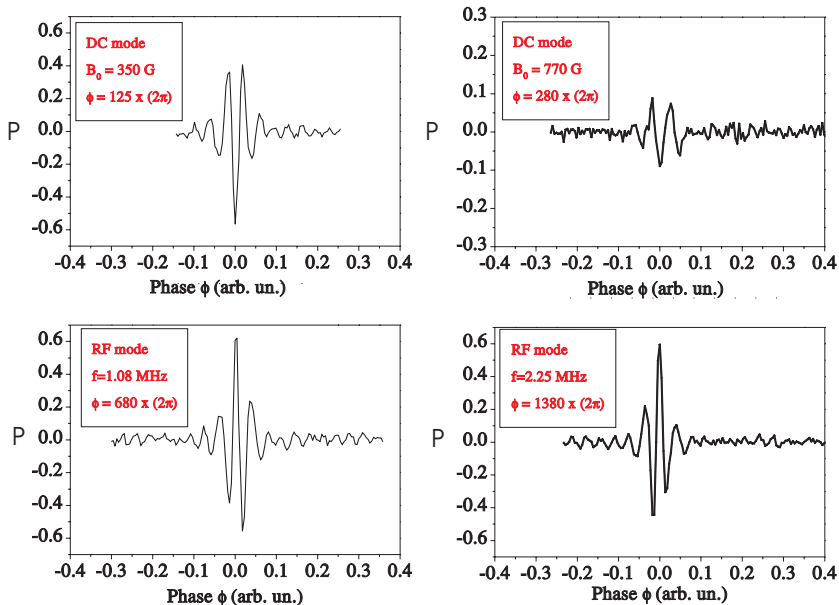


Fig. 16. Spin echo measurements in DC-mode and resonance mode showing the difference in depolarization in these modes. The two top curves correspond to the DC-mode at two different field strengths in the magnets. The bottom two curves correspond to the resonance modes. Note the difference in precession angles in the two modes.

Conclusions

It is possible to build a Larmor precession device with magnetic pole faces, reducing in this way the amount of material in the beam. However, line integral corrections are needed in such geometries. Various options of inclined precession regions have been considered with their characteristics concerning useful wavelength range and corrections for field line integrals. Some basic formulas for line integral deviations have been derived. The corrections can be minimal using π flippers in the main fields of the precession, creating a symmetry plane around which field integral deviations are averaged out. The neutron spin resonance method uses the effect of the π flippers already intrinsically.

Acknowledgement

This work is part of the research programme of the ‘Stichting voor Fundamenteel Onderzoek der Materie (FOM)’, which is financially supported by the ‘Nederlandse Organisatie voor Wetenschappelijk Onderzoek (NWO)’.

References

1. M. Th. Rekveldt, W. G. Bouwman, W. H. Kraan, S. Grigoriev, O. Uca, see contribution in this volume

2. W.G. Bouwman, M. van Oossanen, O. Uca, W.H. Kraan, M.Th. Rekveldt, *J. Appl. Cryst.* **33**, 767 (2000)
3. M. van Oossanen, W.H. Kraan, W.G. Bouwman, M.Th. Rekveldt, *Physica B* **276**, 134 (2000)
4. P. Hank, M. Köppe, R. Gähler, T. Keller, R. Golub, in *Proc. 3rd Summerschool on Neutron Scattering*, Magn. Neutron Scattering, ed. by A. Furrer (World Scientific, Singapore, 1995) p. 228
5. T. Keller, R. Gähler, H. Kunze, R. Golub, *Neutron News* **6**, 16 (1995)
6. R. Golub, R. Gähler, *Phys. Lett. A* **123**, 43 (1987)
7. S.V. Grigoriev, W.H. Kraan, F.M. Mulder, M.Th. Rekveldt, *Phys. Rev. A* **62**, 63601 (2000)
8. O. Uca, W.G. Bouwman, W.H. Kraan, M.Th. Rekveldt, *Physica B* **276**, 136 (2000)
9. O. Uca, W.G. Bouwman, W.H. Kraan, M.Th. Rekveldt, *Physica B* **297**, 28 (2001)